Laminar convective heat transfer characteristics in a 180-degree U-bend of triangular cross section using nanofluid (Accepted).

Conference Paper · October 2016

Bishnu Narayan Mahapatra
Odisha University of Technology and Research Bhubaneswar (Formerly CET Bhubaneswar)

Laminar convective heat transfer characteristics in a 180-degree U-bend of triangular cross section using nanofluid

Adarsh Vasa[1], Ashok K Barik[2*], Bishnu N Mahapatra[3]
[1, 2*, 3] Department of Mechanical Engineering,
College of Engineering and Technology,
Bhubaneswar, 751029, Odisha, India.
E-mail: ashokbarik.mech@gmail.com
(or) ashok_iit@hotmail.com

***Abstract*—Convective heat transfer rate has been quantified for a three dimensional computational domain using Al_2O_3−water nanofluid under different boundary conditions. A triangular duct with 180−degree bend has been chosen. The governing equations have been solved numerically employing commercial code of Fluent 16. The Reynolds number and nanofluid volume fraction have been varied in the range of 1,000-2,000 and 0%-5%, respectively. It has been observed that the heat transfer rate is a strong function of both Reynolds number and nanofluid volume fraction. The peripheral walls of the bend portion have been applied with constant temperature boundary conditions. It has been noticed that when wall-3 is applied with constant temperature, the Nusselt number is higher than the case when wall-1 is applied with constant temperature.**

Keywords— Nanofluid; laminar flow; U-bend; convection

I. INTRODUCTION

Convection is a heat transfer phenomena in which heat is carried out through bulk motion of the fluid. If the thermal conductivity of the fluid medium is increased, it is possible to dissipate more heat from a heated surface to the bulk fluid. Conventional fluids such as oil and water are not able to dissipate more heat due to their low thermal conductivities. Moreover, the heat transfer rate is also affected by the operating conditions, the surface area and velocity of fluid flow. The miniaturization of thermal devices demands elimination of a high heat transfer rate from a small surface area so as to safe guard the devices and to meet the present need of longer durability. Thus, it is challenging to design such devices. Therefore, researchers [1–3] have attempted to optimize the geometry of engineering equipment in order to attain higher thermal efficiency. Also, the focus has been shifted to implement nanofluid as a heat transfer augmenter since it has a high thermal conductivity.

The fluid flow and heat transfer characteristics of a flow containing millimeter and micrometer sized particles have been studied by different researchers [4–7]. Although, the suspended particles cause channel clogging, abrasion of tubes and have poor suspension stability, the high thermal conductivity of these fluids makes them suitable for heat transfer applications [8]. Xuan and Li [9], Wang and Majumdar [10], Kakac and Pramuanjaroenkij [11] studied the heat transfer enhancement of nanofluids. They demonstrated that a higher heat transfer is obtained with the use of nanofluids because of an increased surface area around nanoparticle in the base fluid, thermal conductivity of the suspension, intense particle collision, thermal diffusion and Brownian motion. The effect of nanoparticle size on heat transfer has been studied by Anoop *et al* [12], who reported a better heat transfer enhancement with smaller (45nm diameter) nanoparticle as compared to bigger (150nm diameter) ones. Wen and Ding [13] carried out an experimental investigation for heat transfer characteristics of nanofluids in the developing region of a straight pipe. Also, an experimental investigation of the convective heat transfer enhancement using Al_2O_3/water fluid flowing in a square duct was carried out by Heris *et al* [15]. They concluded that the poor heat transfer performance of a non-circular cross section such as square can be overcome using nanofluids. They also reported that there exists the static fluid region near the corners of the non-circular ducts; and with the use of nanofluid, the nanoparticles can migrate to the sharp corners and effectively dissipate heat from those regions so as to enhance the heat transfer.

From the above literature review, it is evident that research related to heat transfer enhancement in a U-bend duct with triangular cross-section using Al_2O_3 has not been carried out earlier. As far as the authors' knowledge is concerned, this investigation is the first of its kind. Thus, in this study, an attempt has been made, through numerical analysis, to measure the enhancement of heat transfer varying nanofluid volume fraction and Reynolds Number.

II. Mathematical Formulation

A. Physical model and grid arrangement:

An equilateral triangular duct having a 180-degree U-bend has been taken for the present numerical investigation.

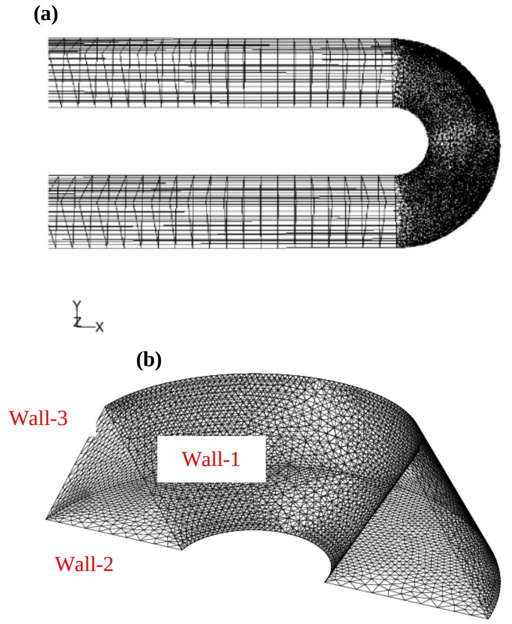

Fig.1. Physical model with grid arrangement **(a);** Expanded and cutaway view of grid arrangement in U-bend **(b)**

The hydraulic diameter (D_h) and the lengths of the approaching and return portions of the duct are 0.03m and $100\times D_h$, respectively. Hexahedral cells have been used for the straight length of duct, while tetrahedral cells are used for the U-bend portion to mesh the computational domain. Thus, a hybrid meshing (Tetrahedral + Hexahedral cells) scheme has been deployed here to control the number of cells in the computational domain. Since the flow would experience a centrifugal force in the U-bend due to curvature effect, fine meshing has been adopted near the walls to capture the sharp gradient in flow variables.

B. Governing equations:

Conservation equations for mass, momentum and energy have been solved iteratively through finite volume technique. Since the size of nano particles is generally less than 100nm, the mixture involving the nanoparticle and base fluid behaves as a continuous medium like a single phase fluid. In this study, the following assumptions have been made:

1. The average flow is steady, laminar and single phase.
2. The slip velocity between nanoparticles and base fluid is negligible, and the thermal equilibrium between the continuous phase and discrete particles is prevailed.
3. The nanofluid is treated as incompressible and Newtonian with constant physical properties. The thermal radiation, viscous dissipation, and compression work are negligibly small in the energy equation. Thus, these terms are neglected.

With the above assumptions, the governing equations are written as follows:

Continuity

$$\rho_{nf}\nabla.v_{nf}=0 \tag{1}$$

Momentum

$$\rho_{nf}\nabla.(v_{nf}v_{nf})=-\nabla p+\nabla.(\bar{\bar{\tau}}) \tag{2}$$

Energy

$$\rho_{nf}C_{p,nf}\nabla.T_{nf}=k_{nf}\nabla.(\nabla T_{nf}) \tag{3}$$

Where $\bar{\bar{\tau}}$ is the stress tensor. Since constant fluid properties have been used in the present study, viscosity and thermal conductivity of the nanofluid have been kept constant.

C. Boundary conditions:

Since Eq. (1) − (3) are elliptic, and nonlinear partial differential equations, an iterative solution method has been adopted to solve the unknown variables by imposing appropriate boundary conditions. At the inlet of the duct, velocity inlet boundary condition has been employed where an axial velocity u_{in} and temperature T_{in}, which is equal to T_o, are specified. The outlet was defined with a pressure outlet boundary condition since atmospheric pressure prevails at the pipe outlet. As the length of the straight channel is 100 times D_h, the flow is expected to be hydro-dynamically fully developed before reaching the U-bend. Here, the approaching and return portions of 180-degree bend are subjected to adiabatic boundary conditions. A constant wall temperature ($T_w=353K$) has been applied to each of the walls 1 and 3 separately. The mathematical descriptions are given as follows:

Pipe Inlet: $$v=w=0, u=u_{in}, T=T_{in}=T_o \tag{4}$$

Pipe Outlet: $$\frac{d()}{dn}=0 \tag{5}$$

Where, n is the outward normal drawn to the pipe outlet.

Adiabatic walls of pipe: $u=v=w=0$

$$\frac{dT}{dx}=\frac{dT}{dy}=\frac{dT}{dz}=0 \tag{6}$$

Constant temperature at U-bend walls: $u=v=w=0$

$$T_x=T_y=T_z=T_w \tag{7}$$

D. Physical properties of nanofluid:

Al_2O_3 nanoparticle when mixed with water is assumed to disperse well with the base fluid, and hence, its thermo-physical properties are evaluated from some well-known classical formulae for single phase, constant property fluids. Different thermo-physical properties of Al_2O_3 nanoparticle and water (i.e., base fluid) are given in the Table 1. The subscripts *p, bf* and *nf* represent the nanoparticle, base fluid and nanofluid, respectively.

TABLE I. THERMO-PHYSICAL PROPERTIES OF Al_2O_3 NANOPARTICLE AND WATER

Properties	Al_2O_3 nanoparticle (*p*)	Water (*bf*)
Density, ρ (kg/m^3)	3880	998.2
Thermal Conductivity, *k* (W/m−K)	36	0.597
Sp. Heat, *c* (J/kg−K)	773	4182
Viscosity (kg/m−s)	–	9.93×10^{-4}

In the present study, temperature independent; volume fraction dependent densities of Al_2O_3−water nanofluid have been used. The equation suggested by researchers [14, 19] for calculation of volume fraction dependent density of nanofluid is given in Eq. (8)

$$\rho_{nf} = (1-\phi)\rho_{bf} + \phi\rho_p \tag{8}$$

Eq. (8) is commonly used to obtain the density of nanofluid, and has been obtained from experimental results of Pak and Cho [20]. The dynamic viscosity of nanofluid was evaluated from the classical homogenous two phase mixture model neglecting the slip velocity between the phases given in Eq. (9)

$$\mu_r = \frac{\mu_{nf}}{\mu_{bf}} = 123\phi^2 + 7.3\phi + 1 \tag{9}$$

The specific heat of the mixture was obtained from Eq. (10) reported by researchers [18, 21-22]

$$c_{nf} = (1-\phi)c_{bf} + \phi c_p \tag{10}$$

The thermal conductivity is determined using Eq. (11).

$$k_f = \frac{k_{nf}}{k_{bf}} = 4.79\phi^2 + 2.72\phi + 1 \tag{11}$$

In Eq. (11), the nanoparticles are assumed as spherical in shape which, in reality, may not be the case. Thus, this model under-predicts the thermal conductivity of nanofluid. However, this model is very simple and easy to implement in numerical computations. That is why we have used it here. The area weighted average Nusselt number, local Nusselt number, bulk mean temperature and the Reynolds number based on hydraulic diameter of duct are given as follows:

The area weighted average Nusselt Number:

$$\overline{Nu} = \frac{1}{A}\int Nu dA. \tag{12}$$

Where, dA is the cross-sectional area

The local Nusselt number:

$$Nu = \frac{h_w D_h}{k_{nf}} \tag{13}$$

where, the local heat transfer coefficient is:

$$h_w = q_w/(T_w - T_b) = (k_{nf}(\partial T/\partial r)\,|\, r=0)/(T_w - T_b) \tag{14}$$

Here, r is the coordinate direction in y and z.

The bulk mean temperature in the computational domain is computed from the local temperature T according to the following equation:

$$\mathrm{T}_b = \frac{1}{A}\int T dA \tag{15}$$

All properties are calculated from the bulk mean temperature.

$$\mathrm{Re}_{Dh} = \frac{\rho_{nf} u_{in} D_h}{\mu_{nf}} \tag{16}$$

III. NUMERICAL SOLUTION PROCEDURE

Conservation equations for mass, momentum and energy were integrated over the control volume to yield a set of algebraic equations. The second order upwind scheme was used for the convective terms [16, 17]. The energy equation was solved using the laminar model. SIMPLE (Semi-Implicit Method for Pressure-Linked Equations) algorithm has been employed for pressure–velocity coupling to solve pressure correction equation. The algebraic equations are then solved iteratively using a point implicit (Gauss–Siedel) linear equation solver in conjunction with algebraic multi-grid solver of Fluent 16 by incorporating appropriate boundary conditions. The under relaxation factors (for pressure = 0.3, momentum = 0.7 and energy = 1) were used to update solution variables at the end of each iteration. Thus, the solutions were found to converge, when the residuals resulting from iterative solutions fell between 10^{-5} and 10^{-7} for the momentum and energy equations respectively.

IV. VALIDATION OF NUMERICAL METHODOLOGY

The validation for the present computational methodology has been carried out with the analytical results of Muralidhar and Biswas [23] as well as with the computational results of Chakraborty [24]. The literature in 180-dergree bend tube of triangular cross section is sparse; therefore we decided to validate our numerical scheme with a square duct. It is seen from Fig.2 that the present numerical method agrees well with the results published in open literature. Thus, we derived confidence to use the present numerical scheme for our analysis.

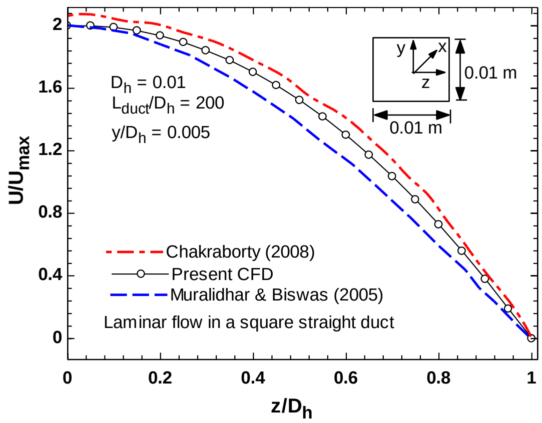

Fig.2. Validation for outlet velocity

V. Results and Discussion

A triangular 180-degree U-bend with a hydraulic diameter of 0.03m and an aspect ratio of 1 is taken into consideration to find the heat transfer of the nanofluid flowing through U-bend. The bent portion of the duct has been meshed with tetrahedral cells with gradual fine mesh in the vicinity of the duct walls so as to capture the sharp change in the gradient of the flow variables. The straight portions of the approaching and return sections have been meshed with hexahedral cells in order to control the number of cells. Thus, a hybrid (i.e., tetrahedral + hexahedral) meshing scheme has been deployed in the present investigation. A grid independence test (see Fig. 3) has been carried out by considering the Reynolds number and nanofluid volume fraction 2,000 and 5%, respectively. Gradual refinement of cells from 75, 515 to 94,406 have been done in the computational domain. As the cells are increased from 75,515 to 92,368, the Nusselt number has been increased by 16.2%, and thereafter, an insignificant change in Nusselt number has been noticed as cells are changed from 92,368 to 94,406. Thus, we declared the domain to be grid independent at 92,368. The grid independent study is carried out by applying constant temperature of 353 K to all the walls of the bend portion only.

Fig. 4 shows the variation of average Nusselt number with the duct Reynolds number as function of nanofluid volume fraction for wall−1 where wall−1 is maintained at constant temperature and all the rest walls are adiabatic. In the same plot, the orientation of the duct walls is shown in the right hand bottom figure. The Reynolds number and volume fraction of nanofluid are varied in the ranges of $1,000 \le \mathrm{Re}_{Dh} \le 2,000$ and $0\% \le \phi \le 5\%$, respectively. It is observed that the Nusselt number increases with the duct Reynolds number for a particular volume fraction. It is quite obvious that the convection strength of the fluid increases with Reynolds number, and thus, enhances the heat transfer from the heated wall to the bulk fluid leading to an increment in Nusselt number.

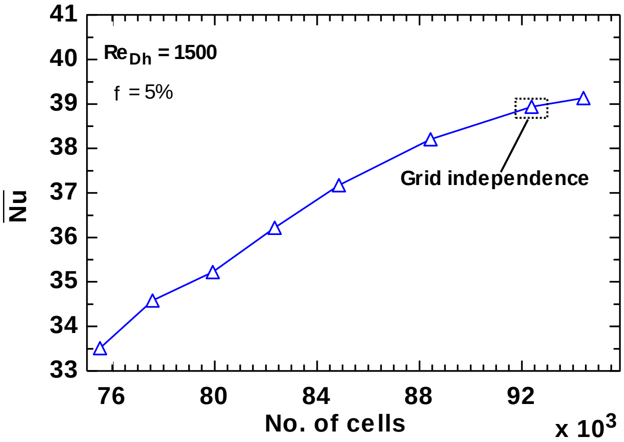

Fig.3. Grid Independence Test

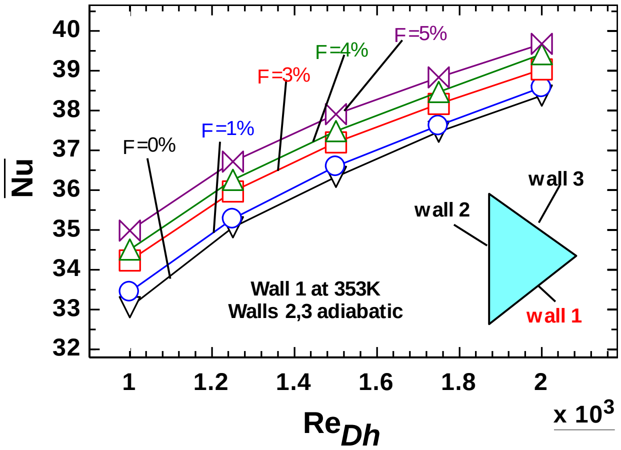

Fig.4. Variation of average Nusselt number with Reynolds number of the duct when Wall 1 at 353 K; walls 2, 3 adiabatic

From Fig. 4, it was found that the Nusselt number increases by 13.4% as Re_{Dh} increases from 1,000-2,000, for $\phi = 5\%$. At a particular $\mathrm{Re}_{Dh} = 2,000$, as the volume fraction increases from 0% − 5%, the Nusselt number is also increased by 3.4%. The addition of the nano-sized particles enhances the thermal conductivity of the suspension (i.e., water + nanoparticle) which can carry more heat from the heated surface to the bulk fluid. Therefore, the Nusselt number increases with increase in nanofluid volume fraction.

Fig. 5 shows the Nusselt number variation with Re_{Dh} as a function of ϕ, when wall−3 is maintained at constant temperature. The Nusselt number, in this case, has been increased by 3.9% as volume fraction increases from 0%-5% at $\mathrm{Re}_{Dh} = 2,000$. A comparison for Nusselt number using different boundary conditions at $\phi = 4\%$ has been shown in Fig. 6. It is quite evident that when wall−3 is maintained at constant temperature the heat transfer enhancement is found to better than the other case. Thus, it is very much essential for the design of the thermal equipment to know the heat transfer enhancement for a better and efficient design.

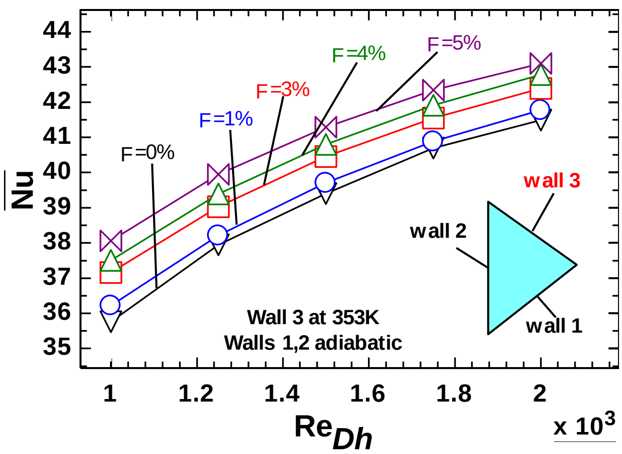

Fig.5. Variation of average Nusselt number with Reynolds number of the duct when Wall 3 at 353 K; Walls 1, 2 adiabatic

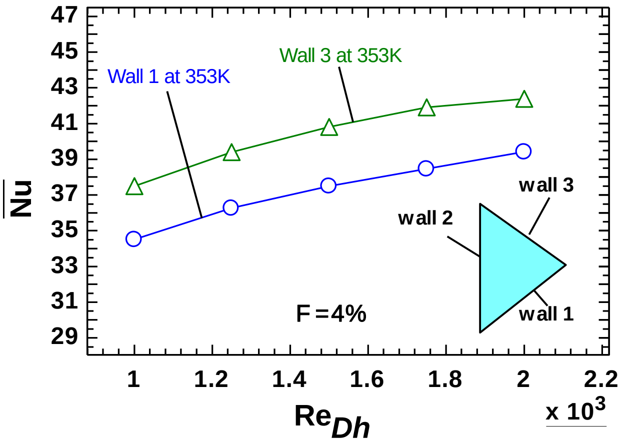

Fig.6. Comparison for heat transfer by two different boundary conditions with ϕ= 4%

VI. Conclusion

Governing equations for mass, momentum and energy are solved in finite volume method with appropriate boundary conditions for a 3-dimensional 180-degree return U-bend pipe in order to reveal the heat transfer characteristics. Water soluble Al_2O_3 nanofluid has been employed for the analysis. Following conclusions can be drawn from the present study.

1. The Nusselt number increases with the duct Reynolds number irrespective of the nanofluid volume fraction.
2. It has been observed that the heat transfer rate is increased with nanofluid volume fraction.
3. When wall-3 is maintained at constant temperature, the heat transfer was found to better that the case where wall-1 is maintained at constant temperature.

List of symbols:

D_h	Hydraulic diameter of the rectangular duct (m)
c_p	Specific heat (J kg^{-1} K^{-1})
k	Thermal conductivity (W m^{-1} K^{-1})
u_{in}	Inlet velocity (m s^{-1})
u, v, w	Velocity in x-, y-and z-directions (m s^{-1})
P	Pressure (N m^{-2})
T_w	Wall temperature (K)
T_0	Inlet temperature (K)
T_b	Bulk mean temperature (K)
$\overline{Nu}$	Area weighted average Nusselt number
Re_{Dh}	Duct Reynolds number based on hydraulic diameter of the duct
q_w	Heat flux of isothermal surface (W m^{-2})

Greek symbols:

ρ	Density (Kg m^{-3})
μ	Kinematic viscosity (N s m^{-2})
ϕ	Volume fraction

Subscripts:

w	Wall
b	Bulk
in	Inlet
o	Outlet
bf	Base fluid
nf	Nano fluid

References

[1] Bejan A and Lorente S 2001 Thermodynamic optimization of flow geometry in mechanical and civil engineering. J. Non-Equilibr. Thermodyn. 26: 305–354

[2] Li Z, Mantel S C and Davidson J H 2005 Mechanical anal-ysis of streamlined tubes with non–uniform wall thickness for heat exchangers. J. Strain Anal. Eng. Des. 40: 275–285

[3] Najafi H and Najafi B 2000 Multi-objective optimization of a plate and frame heat exchanger via genetic algorithm. Heat Mass Transfer 46: 639–647

[4] Ahuja A S 1975 Augmentation of heat transfer in laminar flow of polystyrene suspension. J. Appl. Phys. 46: 3408–3425

[5] Liu K V, Choi S U S and Kasza K E 1998 Measurement of pressure drop and heat transfer in turbulent pipe flows of particulate slurries. Argonne National Laboratory Report ANL-88 15

[6] Roco M C and Shook C A 1983 Modelling of slurry flow: the effect of particle size. Canadian J. Chem. Eng. 61:494–503

[7] Sohn C W and Chen M M 1981 Microconvective thermal conductivity in dispersed two-phase mixture as observed in low velocity Couette flow experiment. J. Heat Transfer 103: 47–51

[8] Choi S U S, Zhang Z G, Yu W, Lookwood F E and Grulke E A 2001 Anomalously thermal conductivity enhancement in nanotube suspension. Appl. Phys. Lett. 79: 2252–2254

[9] Xuan Y and Li Q 2000 Heat transfer enhancement with nanofluids. Int. J. Heat Fluid Flow 21: 58–64

[10] Wang X and Majumdar A S 2007 Heat transfer character-istics of nanofluids: A review. Int. J. Therm. Sci. 46: 1–19

[11] Kakac¸ S and Pramuanjaroenkij A 2009 Review of convective heat transfer enhancement with nanofluids. Int. J. Heat Mass Transfer 52: 3187–3196

[12] Anoop K B, Sundararajan T and Das S K 2009 Effect of particle size on the convective heat transfer in nanofluid in the developing region. Int. J. Heat Mass Transfer 52: 2189–2195

[13] Wen D and Ding Y 2004 Experimental investigation into convective heat transfer of nanofluids at entrance region under laminar flow conditions. Int. J. Heat Mass Transfer 47: 5181–5188

[14] Bianco V, Chiacchio F, Manca O and Nardini S 2009 Numerical investigation of nanofluids forced convection in circular tubes. Appl. Therm. Eng. 29: 3632–3642

[15] Heris S Z, Nassan T H, Noie S H, Sardarabadi H and Sar-darabadi H 2013 Laminar convective heat transfer of Al_2O_3/water nanofluid through square cross section duct. Int. J. Heat Fluid Flow 44: 375–382

[16] Lotfi R, Saboohi Y and Rashidi A M 2010 Numerical study of forced convective heat transfer heat transfer of nanofluids: Comparison of different approaches. Int. Commun. Heat Mass Transfer 37: 74–78

[17] Azari A, Kalbasi M and Rahimi M 2014 CFD and experi-mental investigation on the heat transfer characteristics of alumina nanofluids under the laminar regime. Braz. J. Chem. Eng. 31: 469–481

[18] Maiga S E B, Palm S J, Nguyen C T, Roy G and Galanis N 2005 Heat transfer enhancement by using nanofluids in forced convection flows. Int. J. Heat Fluid Flow 26: 530–546

[19] Akbarinia A and Behzadmehr A 2007 Numerical study of laminar mixed convection of nanofluid in horizontal curved tubes. Appl. Therm. Eng. 27: 1327–1337

[20] Pak B C and Cho Y I 1998 Hydrodynamic and heat transfer study of dispersed fluids with submicron metallic oxide particles. Exper. Heat Transfer 11: 151–170

[21] Mansour R B, Galanis N and Nguyen C T 2007 Effect of uncertainties in physical properties on forced convection heat transfer with nanofluids. Appl. Therm. Eng. 27: 240–249

[22] Barik A K, Satapathy P K and Sahoo S S 2016 CFD study of forced convective heat transfer enhancement in a 90-degree bend duct of square cross section using nanofluid. Sadhana Vol. 41, No. 7,pp. 795–804

[23] Muralidhar K and Biswas G 2005 Advanced engineering fluid mechanics. Norosa Publishing House, New Delhi

[24] Chakraborty G 2008 A note on methods for analysis of flow through microchannels. Int. J. Heat Mass Transfer 51: 4583–458